Respiratory Motion Compensation with Topology Independent Surrogates

Christoph Jud[1], Frank Preiswerk[2] and Philippe C. Cattin[1]

[1]Department of Biomedical Engineering, University of Basel
[2]Brigham and Women's Hospital, Harvard Medical School
{christoph.jud,philippe.cattin}@unibas.ch

Abstract. We present a method for organ motion compensation based on a statistical motion model. The novelty of our method is, that the surrogates for prediction can be independent of the model's topology i.e. the surrogate signal does not have to correspond to a point of the motion model. By non-linear regression, we grasp the correlation between a captured signal during free breathing and the motion model parameters. Such a signal could be a spirometer, a breathing belt or an abdominal ultrasound signal. Our method performs on par with state-of-the-art methods, where model points have to be tracked. However, we solely incorporate one-dimensional and even topology independent surrogates. In our experiments on the right liver lobe we have achieved an average motion prediction accuracy of 2-3mm using population models and below 1mm with patient specific models.

1 Introduction

Respiratory organ motion compensation is central in image-guided thoracical and abdominal interventions. Especially in dynamic dose delivery methods as in radiotherapy or in high intensity focused ultrasound, tumor localization is crucial. Typically, a motion model is used to predict the organ motion given some external respiratory signal (surrogates). Thus, the treatment of healthy tissue can be reduced.

A prominent class of methods [3,7] is based on statistical motion models of organ shape deformations. During treatment, the shape deformation is inferred based on detected points in ultrasound (US) images which serve as surrogates. However, obtaining such surrogates is difficult, since they have to correspond to specific points in the model.

In this paper, we present a statistical motion model in which surrogates are incorporated that originate from arbitrary signal sources provided that they are correlated to the organ motion. For breathing, these might be a spirometer, a breathing belt or a 1D US where the sensor is placed on the abdominal skin [10]. The key idea is to predict the statistical motion model parameters given these surrogate signals using non-linear regression. This greatly simplifies the treatment setup since the absolute position of the surrogate sensor is no longer needed.

Beside the motion prediction, our method enables the synthesis of a respiratory cycle with a high temporal resolution. This can be used to investigate the patient specific motion pattern for planning. Further, in contrast to standard statistical motion model approaches, we construct our motion model with a different number of temporal samples per individual, to make full use of the training data. Finally, the dense underlying shape model opens the possibility to automatically fit the model into the 3D volume. However, this is not in the focus of the present paper.

In our experiments, we study the respiratory motion of the right liver lobe. To predict the organ motion, as surrogates, we simulate a correlated signal to the liver's motion. As such, we have reached an average accuracy between 2 and 3mm using a population based model. Using patient specific motion models, we have reached an accuracy of less than 1mm. The influence of organ drift [11] or rotations caused by change in posture during treatment has not been investigated.

Previously, [7] presented a statistical motion model, where physical points on the diaphragm serve as surrogates which correspond to points in the model. They detected and tracked such points using lateral US images. In [10], a low-cost 1D US signal has been proposed. As surrogate data, they map the US signal to positions on the organ. In our experiments, the depth of the diaphragm is simulated in the view to capture the signal from such a 1D US sensor which is placed on the abdominal skin. A comprehensive review on respiratory motion models can be found in [6].

The estimation of relationships among random variables has priorly been shown in [2] with the application to attribute manipulation in 3D face models. There, regression analysis of facial attributes and face models have been studied. However, to our best knowledge, such an approach has previously *not* been established in clinical applications.

2 Materials and Methods

2.1 Shape Modeling

For each volunteer v, we have a 4DMRI sequence of τ^v time steps, stacked by the method of [12], resulting in τ^v times an MR image $I_t^v : \Omega \to \mathbb{R}$ where $\Omega \subset \mathbb{R}^3$ is the image domain and I_t^v denotes the image at a time point t. For each volunteer, an exhalation master image $I_{t=m}^v$ is selected which serves as reference to determine relative displacements to each other time point. By non-rigid free form registration [9] of the exhalation master to each other image of this volunteer $I_{t\neq m}^v$ the displacement fields $D_t^v : \Omega \to \mathbb{R}^3$ are derived. To deal with across organ boundaries the surrounding of the liver structure is masked out during registration.

The liver structure within each exhalation master image has been manually segmented yielding a label map $L : \Omega \to \{0, 1\}$ which indicates liver structure when $L(x) = 1, x \in \Omega$. Using margin cubes, for each label map a shape $S \subset \mathbb{R}^3$

is obtained. We perform an iterative group-wise registration of the shapes to reduce a bias of the mean shape $\bar{S}$ to a specific exhalation master shape S^v.

$$\bar{S}_1 = S^{v=m}, \quad \bar{S}_{i+1} = \frac{1}{V}\sum_v \bar{S}_i + \Delta S_i^v, \tag{1}$$

where m is randomly chosen and ΔS_i^v is obtained by the Gaussian process registration method of [5] such that $\bar{S}_i + \Delta S_i^v \approx S^v$. In the following, by S^v we always mean the registered shapes $\bar{S} + \Delta S^v$, if nothing else is mentioned.

We equidistantly sample inside of $\bar{S}$ and with thin-plate-spline interpolation we add several interior points to each S^v. To recap, for each volunteer we have now an exhalation master shape S^v, which is in correspondence with the population mean shape $\bar{S}$. By the displacement fields $F_t^v := D_t^v(S^v)$ induced by motion, for each time point we derive a shape $S_t^v := S^v + F_t^v \subset \mathbb{R}^3$ with 2571 surface and 368 interior points.

2.2 Statistical Shape Model

We distinguish between the modeling of shape and the modeling of shape motion. In the shape model, the variation among a population of shapes originating from different individuals is considered. Whereas in the motion model, the shape deformation over time relative to a reference shape is investigated.

For each volunteer v, we have a segmented exhalation master shape S^v of the right liver lobe. The exhalation master shapes, which were brought into correspondence (Equation 1), are assumed to be Gaussian distributed $p(S^v|S_\mu, \Sigma_S) \sim \mathcal{N}(S\mu, \Sigma_S)$ where

$$S_\mu = \frac{1}{V}\sum_v S^v \mathrel{\widehat{=}} \bar{S}, \quad \Sigma_S = \frac{1}{V-1}\sum_v (S^v - S_\mu) \otimes (S^v - S_\mu) \tag{2}$$

are the maximum likelihood estimates of $p(S^v|S_\mu, \Sigma_S)$, V is the number of volunteers and $\otimes$ is the outer-product. Thus, a shape can be parametrized by $S^\alpha = S_\mu + \sum_{i=1}^M \alpha_i \psi_i$, where ψ_i are orthogonal basis vectors of Σ_S weighted by the model parameters α_i and M denotes the number of basis vectors.

2.3 Statistical Motion Model

In addition to the shape variation among a population we model the relative shape deformation over time. Since each volunteer has been observed for a different amount of time, we assume that the displacements are a mixture of Gaussian distributions

$$p(F) = \sum_v^V p(v)p(F|v) = \sum_v^V \pi^v p(F|v), \tag{3}$$

where $\sum_v^V \pi^v = 1, \pi^v \in (0,1), \forall v = 1, ..., V$. Each component distribution is assumed to be Gaussian $p(F^v) \sim \mathcal{N}(F_\mu^v, \Sigma_{F^v})$ with

$$F_\mu^v = \frac{1}{\tau^v}\sum_t^{\tau^v} F_t^v, \quad \Sigma_{F^v} = \frac{1}{\tau^v - 1}\sum_t^{\tau^v} (F_t^v - F_\mu^v) \otimes (F_t^v - F_\mu^v). \tag{4}$$

The first two moments of the mixture $p(F)$ are estimated by

$$F_\mu = \sum_v^V \pi^v F_\mu^v, \quad \Sigma_F = \sum_v^V \pi^v \left(\Sigma_{F^v} + \left(F_\mu^v - F_\mu\right) \otimes \left(F_\mu^v - F_\mu\right)\right), \tag{5}$$

where $\pi^v = \tau^v / \sum_v^V \tau^v$ is the weighting of the component distribution with respect to the number of temporal samples per volunteer (see more details about moments of Gaussian mixtures in [4])

The variation of the shape displacements is finally parametrized by $F = F_\mu + \sum_{i=1}^N \beta_i \phi_i$, where ϕ_i are N orthogonal basis vectors of Σ_F.

With the combination of the shape and the motion model a shape to a particular time point can be synthesized by

$$S_\beta^\alpha = \underbrace{S_\mu + \sum_{i=1}^M \alpha_i \psi_i}_{\text{shape model}} + \underbrace{F_\mu + \sum_{i=1}^N \beta_i \phi_i}_{\text{motion model}}, \tag{6}$$

where α_i and β_i are coefficients of the shape and the motion model respectively. Typically, the shape model is priorly fitted to an exhalation master shape [5]. Subsequently, the shape motion is additively imposed to the derived shape.

2.4 Attributes and Regression

Let $a \in \mathbb{R}^d$ be a d-dimensional attribute vector which corresponds to a particular time point. Consider an observed finite set $A = \{(a_0, \beta_0), ..., (a_n, \beta_n)\} \subset \mathbb{R}^d \times \mathbb{R}^N$ of n pairs of i.i.d. attribute vectors a_i and motion coefficient vectors β_i. Let further assume that there exists a function $f : \mathbb{R}^d \to \mathbb{R}^N$ which maps the attribute vectors to the coefficient vectors, while we only observe noisy instances of β such that $\beta \sim \mathcal{N}(f(a), \sigma_\epsilon \mathbf{I})$.

Gaussian Process Regression Let $f \in \mathcal{GP}(0, k)$ be a Gaussian process with the covariance function $k : \mathbb{R}^d \times \mathbb{R}^d \to \mathbb{R}$. Assuming a Gaussian likelihood, the posterior distribution $p(f|A)$ is given in closed form [8] and is again a Gaussian process $\mathcal{GP}(\mu_A, k_A)$ with

$$\mu_A(a) = \mathbf{K}_{a,A}^T (\mathbf{K}_{A,A} + \sigma_\epsilon \mathbf{I})^{-1} \mathbf{B} \tag{7}$$

$$k_A(a, a') = k(a, a') - \mathbf{K}_{a,A}^T (\mathbf{K}_{A,A} + \sigma_\epsilon \mathbf{I})^{-1} \mathbf{K}_{a',A}, \tag{8}$$

where $\mathbf{K}_{a,A} = (k(a_i, a))_{i=1}^n \in \mathbb{R}^n$, $\mathbf{K}_{A,A} = (k(a_i, a_j))_{i,j=1}^n \in \mathbb{R}^{n \times n}$ and $\mathbf{B} = (\beta_0, \ldots, \beta_n)^T \in \mathbb{R}^{n \times N}$. The expectation of an unseen output β^* given an attribute a^* yields Equation 7.

In our application, we use a straight forward Gaussian process model, where we apply a Gaussian kernel as covariance function

$$k_g(x, x') = \theta_0^2 \exp\left(-\frac{\|x - x'\|^2}{2\theta_1^2}\right), \tag{9}$$

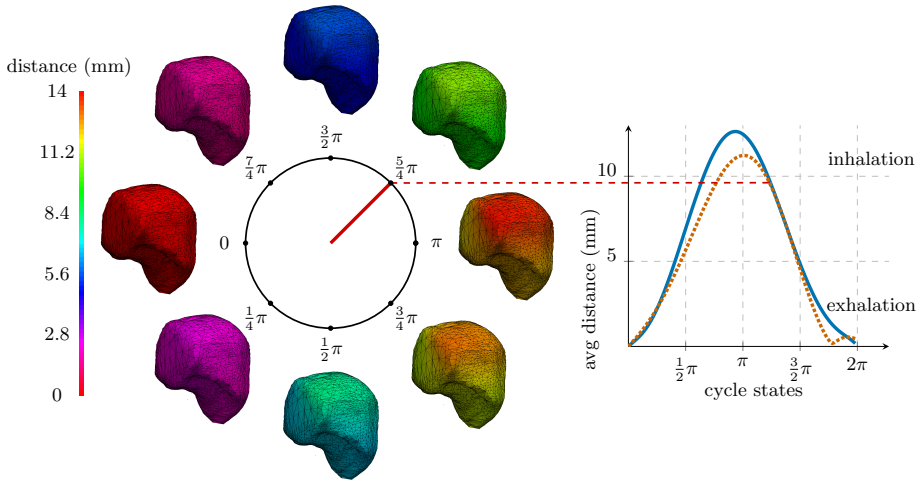

Fig. 1: Example liver shape S^v deformed by an average respiratory cycle $c = [0, 2\pi]$. The shape is colored with respect to the absolute value of the displacement of a point $|\Delta p| \in [0, 14]$ mm. In the right plot, the average distance to the exhalation master is plotted (*blue* - population mean, *orange dotted* example of a patient specific cycle).

where θ_0 is a scaling parameter and θ_1 is a length scale or smoothness parameter.

Given an attribute signal which is correlated with the organ motion, we have defined now the tools to predict the motion model parameters β of the current respiratory state with Equation 7. Based on that, a shape deformation can be synthesized using Equation 6.

In the following, we first synthesize a high-temporal resolution respiratory cycle. This is followed by the evaluation of the prediction performance of our method.

3 Results

3.1 Average Breathing Cycle

In this first study, we analyze the respiratory motion of the liver in general. We built a motion model out of the motion samples among all the $V = 9$ volunteers, while we have kept 99.9% of the variance. For each sample shape S_t, an attribute $c \in [0, 2\pi]$ has been considered which indicates the cycle state of t within a respiratory cycle[1]. This rather abstract attribute is applied to synthesize an average respiratory cycle of the liver shape. For the regression, 8 000 pairs

[1] This cycle attribute was computed using a greedy cycle detection algorithm which is based on the average vertical coordinates of the displacement fields F_t.

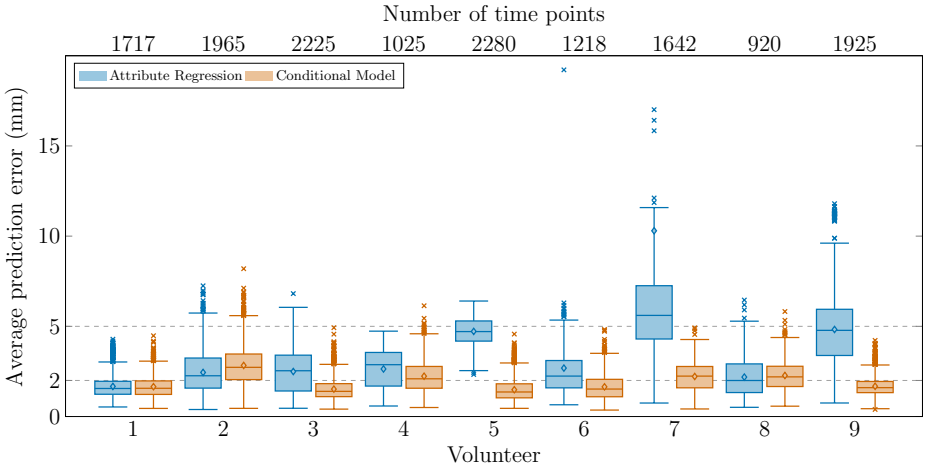

Fig. 2: For each L1O experiment, the average corresponding point difference between the ground truth and the predicted shape is visualized. We compare our method *Attribute Regression* with the *Conditional Model* [1,7]. The upper x-axis indicates for how many time points the motion has been predicted.

of cycle attributes resp. motion model coefficients have been randomly picked among all volunteers.

In Figure 1, an example right liver lobe and its displacements within this average respiratory cycle is visualized. Note that here, we synthesize a semantic and non-linearly captured respiratory cycle of a shape, where we do *not* simply vary the most dominant principal component of the motion model. Thus, for each patient we can generate an average respiratory cycle e.g. for planning. While the source 4DMRI has a framerate of 2.8Hz the temporal resolution can be arbitrary high. In this example, 100 samples have been synthesized which corresponds to approximately 25Hz.

3.2 Motion Model Prediction

In the motion prediction experiment, we simulate a surrogate signal which indicates the depth of the diaphragm measured from the abdominal skin for example by a 1D US sensor. We define a 1D signal which is generated by a ground truth model point in the region of the diaphragm. Let $s : [0, \tau] \to \mathbb{R}^3$ be the 3D signal of absolute coordinates of this point at time point $t \in [0, \tau]$. To get invariant to the absolute positioning of the patient lets project the signal into its dominant mode of variation

$$\mathcal{F}[s] = (s - \mu_s)\psi_0 + \epsilon, \tag{10}$$

where $\mu_s = \frac{1}{\tau}\int_0^\tau s(t)\mathrm{d}t$ is the signal mean value, $\epsilon \sim \mathcal{N}(0, \sigma_\epsilon)$ is additive noise, which has been set to $\sigma_\epsilon = 2$mm and ψ_0 is the orthonormal eigenfunction corre-

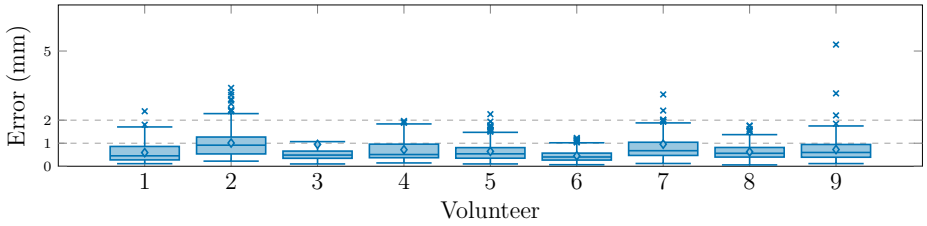

Fig. 3: Evaluation of the average prediction error for each patient specific experiments, where $\theta_1 = 5$, 700 training samples have been picked and 210 tests have been performed.

sponding to the largest eigenvalue λ_0 of the equation $\int_0^\tau \mathrm{cov}(s_i, s_j)\psi_0(s_i)\mathrm{d}s_i = \lambda_0\psi_0(s_j)$. Here, cov is the covariance function of the signal s.

In this evaluation, we show the motion prediction performance of our method given the simulated signal $\mathcal{F}[s]$. For each volunteer, we generated a leave-one-out (L1O) motion model, where only motion samples from the other volunteers have been considered. 99.9% of the variance has been kept yielding L1O-models of 20 to 22 principal modes. Note that for each sample, we additionally computed $\mathcal{F}[s]$ for the later usage as an attribute (Equation 10).

For the Gaussian process regression, we randomly picked 8 000 $\mathcal{F}[s]$-attributes resp. ground truth coefficient vector pairs, again only from the other volunteers. We manually optimized the parameters and used $\theta_1 = 3$, while the exact value of $\theta_0 = 5\,000$, had only minor influence to the prediction performance. In Figure 2, for each volunteer the average prediction error is plotted. The prediction error is robustly kept below 5mm, whereas the median stays around 2 to 3mm. For radiotherapy these are reasonable error bounds.

We compare our method to [7] where the simulated 3D point signal s serves as surrogate data. The prediction is performed by estimating the mean of a statistical motion model which is conditioned on s [1]. For a fair comparison, we added to s an isotropic Gaussian noise $\mathcal{N}(0, \sigma_\epsilon/\sqrt{3})$. The conditional model performs equally well, while it better generalizes in the experiment with volunteer 7 and 9. Certainly, our model with only 9 volunteers is not capable to generalize to the respiratory motion of these two subjects. This can be confirmed when comparing to the results with patient specific models (Figure 3). Here, for each volunteer, we built a motion model where only samples from the volunteer of interest are considered. For the regression, 700 attribute/coefficient pairs have been randomly picked and we adjusted $\theta_1 = 5$. For all volunteers including for volunteer 7 and 9, the average error has been considerably improved to less than 1mm. In Figure 1 on the right, a patient specific average respiratory cycle is plotted for a comparison to the population mean cycle.

4 Conclusion

We have presented a new method for organ motion compensation based on a statistical motion model, in which the surrogate data can be independent of the model's topology. The major novelty of our method is the non-linear regression of the surrogate data and the model parameters. Although already a simple Gaussian process model yields reasonable results the potential of our method is far from being exhausted. The regression is *not* limited to one attribute and will gain robustness and precision with additional surrogate sources as e.g. 2D US data. Further, we will investigate more complex and combined covariance functions and a full Gaussian process inference to obviate parameter selection. In the experiments, we have shown a reasonable prediction performance using population based models. The generalization of the respiratory motion was further improved by a patient specific regression as shown in the last experiment.

References

1. Albrecht, T., Lüthi, M., Gerig, T., Vetter, T.: Posterior shape models. Medical image analysis 17(8), 959–973 (2013)
2. Amberg, B., Paysan, P., Vetter, T.: Weight, sex, and facial expressions: On the manipulation of attributes in generative 3d face models. In: Advances in Visual Computing, pp. 875–885. Springer (2009)
3. Boye, D., Samei, G., Schmidt, J., Székely, G., Tanner, C.: Population based modeling of respiratory lung motion and prediction from partial information. In: SPIE Medical Imaging. pp. 86690U–86690U. International Society for Optics and Photonics (2013)
4. Carreira-Perpiñán, M.Á.: Mode-finding for mixtures of gaussian distributions. IEEE Transactions on Pattern Analysis and Machine Intelligence 22(11), 1318–1323 (2000)
5. Lüthi, M., Jud, C., Vetter, T.: A unified approach to shape model fitting and non-rigid registration. In: Machine learning in medical imaging, pp. 66–73. Springer (2013)
6. McClelland, J.R., Hawkes, D.J., Schaeffter, T., King, A.P.: Respiratory motion models: A review. Medical image analysis 17(1), 19–42 (2013)
7. Preiswerk, F., Arnold, P., Fasel, B., Cattin, P.C.: A bayesian framework for estimating respiratory liver motion from sparse measurements. In: Abdominal Imaging. Computational and Clinical Applications, pp. 207–214. Springer (2012)
8. Rasmussen, C.E.: Gaussian processes for machine learning (2006)
9. Rueckert, D., Sonoda, L.I., Hayes, C., Hill, D.L., Leach, M.O., Hawkes, D.J.: Non-rigid registration using free-form deformations: application to breast mr images. Medical Imaging, IEEE Transactions on 18(8), 712–721 (1999)
10. Schwartz, B.M., McDannold, N.J.: Ultrasound echoes as biometric navigators. Magnetic Resonance in Medicine 69(4), 1023–1033 (2013)
11. von Siebenthal, M., Székely, G., Lomax, A.J., Cattin, P.C.: Systematic errors in respiratory gating due to intrafraction deformations of the liver. Medical physics 34(9), 3620–3629 (2007)
12. Von Siebenthal, M., Székely, G., Gamper, U., Boesiger, P., Lomax, A., Cattin, P.: 4d mr imaging of respiratory organ motion and its variability. Physics in medicine and biology 52(6), 1547 (2007)